

Review

The Role of Clay Mineral-Derived Photocatalysts in Insights of Remediation

Walber Freitas ¹, Pollyana Trigueiro ², Thiago Marinho ³, Luzia M. Honorio ⁴, Edson C. Silva-Filho ¹, Marcelo B. Furtini ¹, Juan A. Cecilia ⁵, Maria G. Fonseca ³ and Josy Osajima ^{1,*}

¹ Interdisciplinary Laboratory for Advanced Materials (LIMAV), UFPI, Teresina 64049-550, Brazil

² Materials Science and Engineering Postgraduate Program (PPGCM/CCSST), UFMA, Imperatriz 65900-410, Brazil

³ Research and Extension Center-Fuel and Materials Laboratory (NPE-LACOM), UFPB, João Pessoa 58051-970, Brazil

⁴ Department of Chemistry and Physics, UFPB, Areia 58397-000, Brazil

⁵ Department of Inorganic Chemistry, Crystallography and Mineralogy, University of Malaga, UMA, 29001 Malaga, Spain

* Correspondence: josyosajima@ufpi.edu.br

Abstract: Clay minerals have advantages to be used as supports for obtaining new catalysts, in which colloidal and surface characteristics play a significant role. In addition to their favorable physicochemical properties, clay minerals allow different modifications to form structures with broad photochemical capabilities. This review collects pertinent works of semiconductor nanoparticles loaded onto clay minerals and their potential application in hazardous contaminant photodegradation. Web of Science, Scopus, and Science Direct were used for bibliographic research databases. The sol-gel method is the most frequent technique used to obtain semiconductors immobilized onto clay minerals, but other methods have also proven helpful in forming these structures. Thence, the types of synthesis and different parameters that influence their photocatalytic efficiency will be discussed. Pillared clay minerals have been applied to photo-oxidation reactions involving photodecomposition of environmental contaminants. The homogeneous dispersion of nanoparticles on the surface of clay minerals, reduction of fine particles, its non-toxicity, and the generation of a suitable suspension for photocatalytic reactions may be the main characteristics of these inorganic supports to obtain successful photoactive materials.

Keywords: clay minerals; photodegradation; environmental remediation



Citation: Freitas, W.; Trigueiro, P.; Marinho, T.; Honorio, L.M.; Silva-Filho, E.C.; Furtini, M.B.; Cecilia, J.A.; Fonseca, M.G.; Osajima, J. The Role of Clay Mineral-Derived Photocatalysts in Insights of Remediation. *Ceramics* **2022**, *5*, 862–882. <https://doi.org/10.3390/ceramics5040063>

Academic Editor: Gilbert Fantozzi

Received: 5 September 2022

Accepted: 12 October 2022

Published: 26 October 2022

Publisher's Note: MDPI stays neutral with regard to jurisdictional claims in published maps and institutional affiliations.



Copyright: © 2022 by the authors. Licensee MDPI, Basel, Switzerland. This article is an open access article distributed under the terms and conditions of the Creative Commons Attribution (CC BY) license (<https://creativecommons.org/licenses/by/4.0/>).

1. Introduction

Emerging contaminants (ECs) are compounds used in habitual products, such as personal care products, plasticizers, nutraceuticals, pharmaceuticals, cosmetics, fertilizers and some endocrine disruptors [1]. The presence and control of these pollutants throughout the environment has recently become a global concern, mainly due to adverse effects on the biosphere and humans. They are continuously released into the environment at a slightly increasing rate without monitoring [2,3]. The primary source of ECs is wastewater effluents. However, they are also found in water supply sources, groundwater, and even drinking water. Among the treatment possibilities, alternative processes may be more efficient for removing some pollutants that are difficult to eliminate by conventional methods. Advanced photochemical oxidation processes promote the degradation of pollutants and can mineralize to carbon dioxide, water, or inorganic compounds [4]. Among these, heterogeneous photocatalysis is an economical, environmentally compatible, and suitable method for the environmental protection field [5].

In heterogeneous photocatalysis, when a semiconductor is irradiated with photons whose energy is equal to or higher than their bandgap energy ($h\nu \geq E_g$), these photons are

absorbed. As a result, electron/hole pairs are generated, inducing the formation of free electrons (e^-) in the conduction band and into holes (h^+) in the valence band [6], promoting the formation of reactive species, such as superoxide radicals ($O_2\bullet^-$) and hydroxyl radicals ($OH\bullet$), capable of decomposing pollutants by photochemical reactions, as seen in the scheme in Figure 1. Growing studies using photocatalytic processes have been highlighting the use of different semiconductors as photocatalysts for the removal of various organic or inorganic pollutants in aqueous or gaseous media.

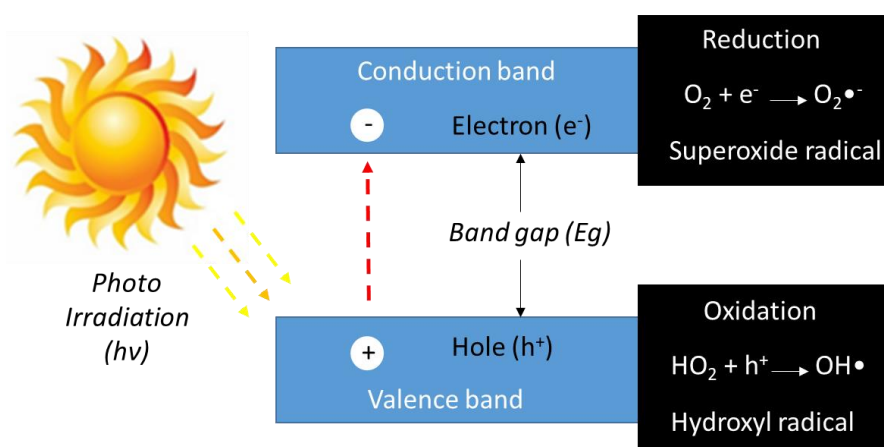


Figure 1. Schematic representation of semiconductor excitation by bandgap illumination generating photoelectrons in the conduction band and photo holes in the valence band.

The photocatalytic activity of materials can be intensely dependent on their structure and physical properties, and the incorporation of dopants or supports are strategies to improve photocatalytic activity. These resources can increase the specific surface area, modify the bandgap, and increase active sites' stability and presence [7]. With the use of some supports, the pre-adsorption of compounds on the surface of support can occur, and this phenomenon should allow the necessary diffusion of the adsorbed substrate and increase the contact with the semiconductor [8]. Different supports can be used to obtain hybrid photocatalysts, for example, oxides [7], graphene [9], activated carbon [10], the polymer [11], or clay minerals [12,13]. Clay mineral-based hybrids have received attention in photocatalytic studies due to the significant increase in photocatalytic activity of these supported semiconductors.

The search was obtained from the Web of Science, Scopus, and Science Direct databases. The investigation was performed without period restriction, including experimental articles and reviews. The primary reference themes used for the systematic search were modified clay minerals applied in photocatalytic studies:

1. Pillared clay minerals;
2. Semiconductors supported on clay minerals;
3. Strategies and synthesis routes for obtaining oxide–clay mineral materials;
4. Properties of oxide–clay mineral-based photocatalysts;
5. Target contaminants treated by semiconductors supported on clay minerals.

The study aims to investigate different materials based on clay minerals, the impact of the processes of obtaining these materials, and the photocatalytic potential for the degradation of emerging contaminants in the solution. Furthermore, to investigate the advantages and challenges of using supported semiconductors and modified clay minerals in photocatalytic applications.

2. Clay Minerals Features

Clay minerals are hydrated phyllosilicates with SiO_4 as their primary structural chemical unit. They consist of a tetrahedral sheet (T) with infinite planes of silica, where the

Al^{3+} or Fe^{3+} species can also be located as the central place of the tetrahedron, and the four oxygen atoms located at the edges. The silicate tetrahedron is connected to the neighboring tetrahedron by basal oxygen 3, forming an undistorted hexagonal structure. In addition to the tetrahedral sheets, the clay minerals have octahedral sheets (O) consisting of edge-sharing $[MO_4(OH)_4]$ units, where M can be a trivalent, divalent, or monovalent cations, and the leading site of octahedron can also be vacant. The tetrahedral sheet can bond to the octahedral sheet, and that condensation of T-O occurs. The result of this condensation is called a “layer” [14,15]. However, all the clay minerals are composed of either TO (Figure 2a) or TOT (Figure 2b) layer models.

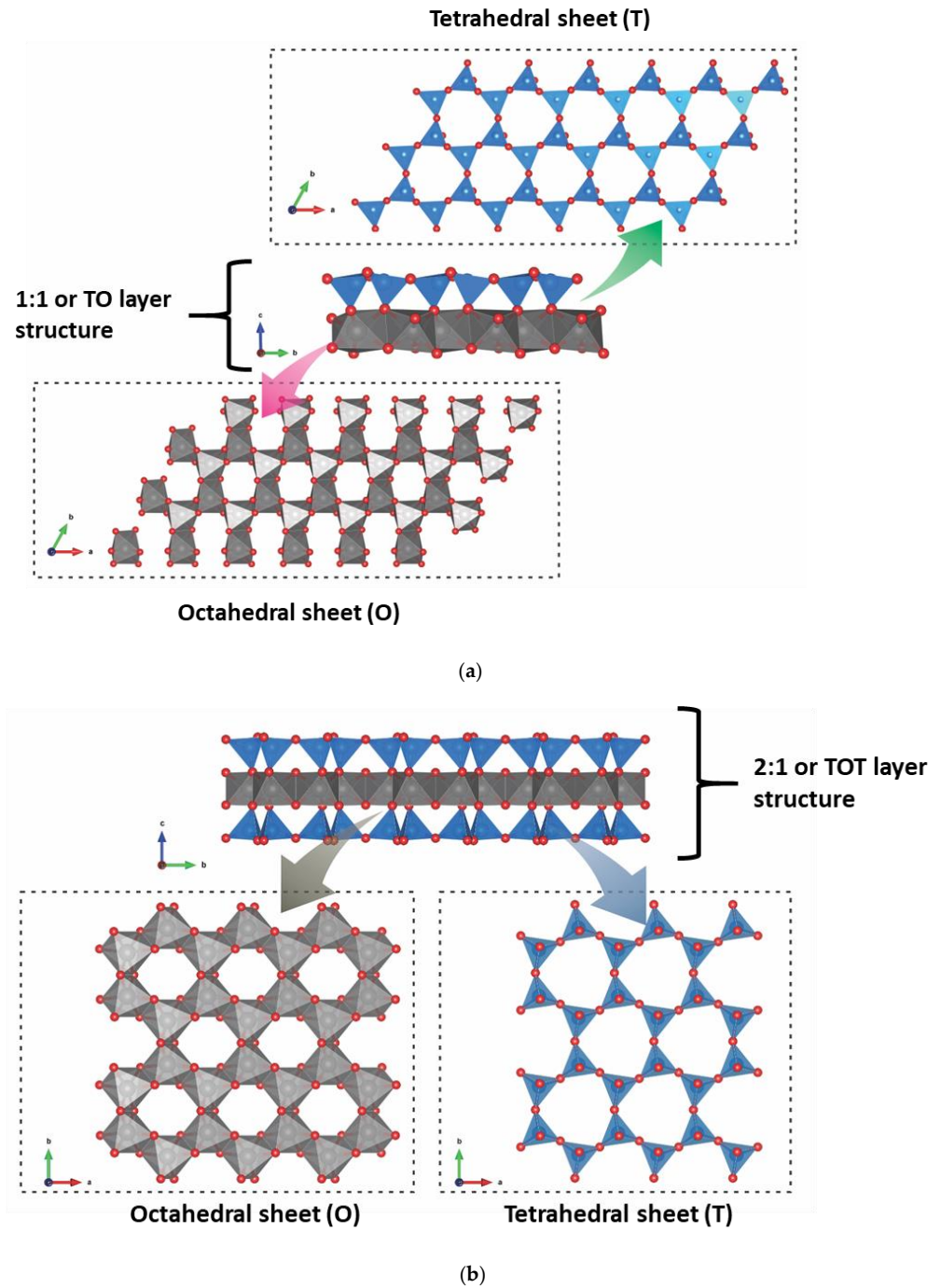


Figure 2. Tetrahedral and octahedral sheets and (a) TO and (b) TOT layers of the clay mineral structures.

Both structures (TO and TOT) can be charge neutral. In this case, they do not have intercalated cations to counterbalance the global lamellar charge, where the superposition of layers can occur through chemical interactions of different natures [15]. Different degrees of isomorphic substitution can occur for the derived clay mineral groups in the T and O sheets of the layers structure. For example, the tetrahedral sheet contains Si^{4+} partially substituted by Al^{3+} or Fe^{3+} cations. In the octahedral sheet, high charge cations are substituted by cations with charges lower by one, such as Al^{3+} by Mg^{2+} , Fe^{2+} or Mg^{2+} by Li^+ . As a consequence, the layers are negatively charged. Cations counterbalance negative charges in the interlayer space to maintain global electric neutrality [14].

As observed, the TO or 1:1 layer structure comprises a tetrahedral sheet linked to an octahedral sheet. In contrast, in the TOT or 2:1 type layer structure, an octahedral sheet is sandwiched between two tetrahedral sheets. A surface of the layer in a 1:1 layer structure is constituted by the basal oxygen of the tetrahedral sheet. The opposite surface is constituted by the oxygen of the octahedral sheet, mainly OH. In the 2:1 layer structure, the two surfaces are constituted by the basal oxygen of the opposing tetrahedral sheets [16].

The adsorption capacity is the competence of clay minerals to interact with dissolved substances through surface forces. There is an increase in the concentration of this substance at the adsorbent interface, and physical and chemical interactions can exist by ionic exchange. The cation exchange capacity (CEC) is defined as the ability of clay minerals to retain cations in the interlamellar spacing, which is directly related to the negative charge of the layers.

Among several clays and clay minerals, some are used in the studies covered in this review.

Smectites have a structure in planar layers of 2:1 (TOT) type, and the lamellar layer charge varies from 0.2 to 0.6 per half-cell unit. Montmorillonite (Mt) is the most widely used clay mineral belonging to this group. Mt is the main component of bentonites (mineral constituted predominantly by $\geq 50\%$ smectite) [17]. In smectites, Si^{4+} and Al^{3+} ions occupy the tetrahedral sites, while Al^{3+} and Mg^{2+} occupy the octahedral sites and interlayer exchangeable cations are usually Na^+ or Ca^{2+} . Hectorite (Hec) is a dioctahedral smectite whose octahedral sheet Mg^{2+} ions, partly substituted with Li^+ , occupy the central place, and Laponite is a trading name for a variety of synthetic hectorites [14].

Vermiculite (Ver) is a 2:1 lamellar clay mineral with a total layer charge between 0.6–0.9 per half-cell unit. Vermiculite has octahedral sheets sandwiched between two silicate tetrahedral sheets, having several different interlamellar cations. The most common form is trioctahedral (structures with six octahedral sites occupied) [18].

Sepiolite (Sep) and palygorskite (Pal) are complex magnesium phyllosilicates that contain a continuous two-dimensional tetrahedral sheet, but the octahedral structure is not continuous, creating an open channel structure. These structures can contain bands or ribbons of 2:1 silicates, forming elongated crystals [16]. These phyllosilicates show a fibrous morphology with channels running parallel to the length of the fiber.

Kaolinite (K) is composed of arranged layers of single tetrahedral and octahedral sheets forming a 1:1 type clay mineral [19]. The rolling of kaolinite-type structure forms halloysite (Hal). Halloysite nanotubes (HNTs) are a widespread clay mineral with interesting chemical properties of external/internal surfaces, facilitating the modification and formation of functional materials [20].

Lamellar double hydroxides (LDH) are referred to as “anionic clays,” and are formed of positively charged brucite-like layers and have attracted a great deal of attention because of their potential applications in adsorption, drug delivery, catalysis, and photocatalysis studies [21].

Clay minerals have different structures and morphologies that provide different adsorption and catalytic support abilities [22–25]. Smectites have a large CEC and a high surface area with unsaturated chemical bonds, presenting great capacity for the adsorption and interactions of contaminants. In contrast, halloysite and palygorskite have moderate CEC and high surface area but have a large pore structure, consequently

having the considerable potential for pollutant adsorption and degradation. Kaolinite has lower adsorption capacity and a smaller surface area than the others, presenting promising results in photocatalytic tests for organic contaminant degradation [26]. Thus, clay minerals are considered very versatile materials since they can obtain surfaces with great reactive capacity.

Clay minerals are abundantly applied in environmental remediation. Thus, it can highlight their use in photocatalytic studies [27,28]. Furthermore, raw clay minerals have been widely employed as supports for incorporating nanoparticles to degrade contaminants in water due to their large reserves, availability, swelling, non-toxicity, and low cost. In this context, a comparative analysis of the different types of clay minerals, morphologies, surface chemistry, trapping potential, and photocatalytic performance will be presented in this review. Furthermore, we will explore the main factors that can influence the photocatalytic activity of semiconductors supported on clay mineral matrices.

3. TiO₂ Supported onto Different Clay Minerals

Researchers highly appreciate the application of TiO₂ in heterogeneous photocatalysis. Titanium dioxide has three polymorphic phases: anatase, rutile, and brookite. However, the anatase phase is the most found in photocatalytic studies because it is the most photoactive phase, even though the rutile phase is thermodynamically stable [29]. TiO₂ is the most used semiconductor in photocatalysis studies, but different semiconductors, including materials such as CdS, WO₃, Fe₂O₃ and ZnO, have sufficient band gap energies for the effective catalysis of many photochemical reactions [30]. When applied in photocatalysis, semiconductors must have specific characteristics: light absorption, suitable band energetics, high charge mobility, long charge carrier diffusion length, intense catalytic activity, good stability, sustainability, and low cost [31]. Sustainability refers to the semiconductors being cheaper, abundant, eco-friendly, and can be obtained by “green synthesis”.

Clay minerals have been widely used in combination with TiO₂ nanoparticles for photocatalytic degradation to improve the removal of organic pollutants in solutions [28,32]. Semiconductor nanoparticles impregnated on the matrix surface can increase the resistance to agglomeration and favor interactions due to possible pre-adsorption of the pollutant. Furthermore, the diffusion of organic solutes provides their effective interaction with nanoparticles and the reactive species generated after light absorption, then TiO₂/clay mineral nanocomposites can lead to increased photocatalytic performance [33]. For example, TiO₂ (anatase) supported on hectorite and kaolinite clay minerals exhibited high photocatalytic efficiency for degradation of two model volatile organic compounds (VOCs), which are commonly present in indoor air: toluene and D-limonene. The authors also observed that the results of photocatalytic activity of the nanocomposites were similar to P25 TiO₂ nanoparticles [33].

Manova et al. [34] prepared titanium dioxide/clay mineral heterostructures from smectites or vermiculite, using a colloidal route, for photocatalytic degradation of 2,4-dichlorophenol. The results indicated that the TiO₂ anatase nanoparticles have good dispersion in the delaminated materials. Furthermore, from the irradiation tests, more excellent photocatalytic activity was observed for the nanocomposites compared to commercial P25 (results compared by per mass of TiO₂), and even the clay mineral-based photocatalysts were more easily recovered from the reaction medium.

Laponite was used to obtain a TiO₂ (anatase) based photocatalyst [35] and applied in the photodegradation of ionic and non-ionic herbicides. The results give the anatase phase crystallization onto the clay mineral lattice. The micrographs confirm the excellent dispersion of the nanoparticles in the delaminated matrix. This study also shows the high photocatalytic performance of TiO₂ supported on mineral clay and the recovery of the photocatalyst. The nanocomposite was highly efficient in the photocatalytic degradation of bromacil, chlortoluron, sulfosulfuron, alachlor, and imazaquin.

The performance of the semiconductor can be optimized using smectites as photocatalytic support, carried out through the incorporation of this mineral with oxide nanoparti-

cles supported within the spacing between layers and/or onto external surfaces. TiO_2 is perhaps the most used semiconductor, but several other photocatalysts have been studied for oxide/clay mineral systems. Figure 3 illustrates the general loading scheme of these oxides in the structure of smectites. Usually, the Ti precursor solution is mixed with a dispersion of clay mineral; after reaction, the solid obtained is calcined for the incorporation of the oxide on the internal and external surface of the support. The connections between TiO_2 nanoparticles and the surface of clay minerals occur when intercalated and/or interacting with the external surface of the support. These interactions can happen by electrostatic forces and likely covalent bonds.

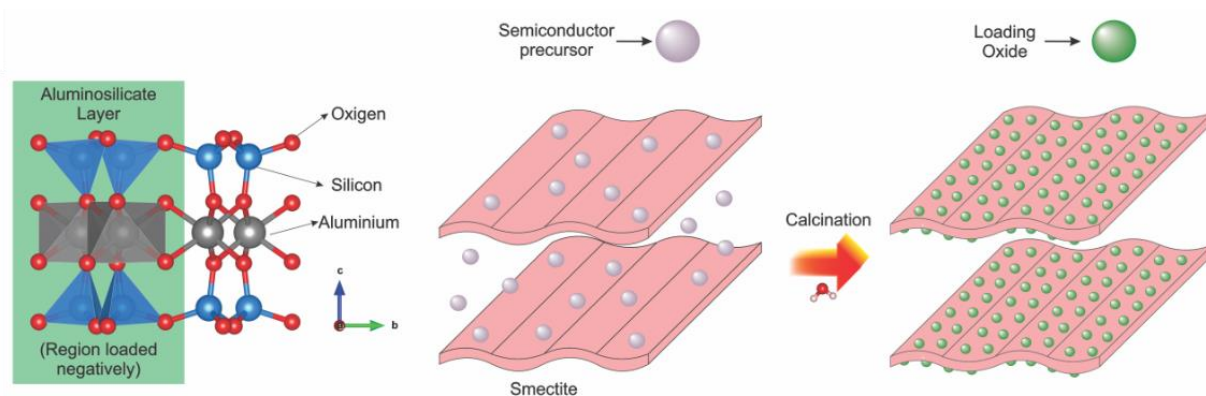


Figure 3. Proposal for the immobilization of different semiconductor oxides in the structure of smectites.

The dispersion of the thin TiO_2 anatase nanoparticles on the tubular surface of the halloysite becomes a strategy to reduce the formation of aggregation of metallic nanoparticles, consequently increasing the photocatalytic activity. The presence of these semiconductors activated by UV light can promote the active area of the nanocomposites and, consequently, the active sites exposed to targeted pollutants [36,37]. Typical nanocomposites obtained by combining TiO_2 nanoparticles and halloysite structures are displayed in Figure 4. The nanocomposite synthesis is performed by combining the clay mineral sample with a Ti precursor solution. Then, heat treatment is required to load the TiO_2 onto the external surface in the halloysite nanotube structure.

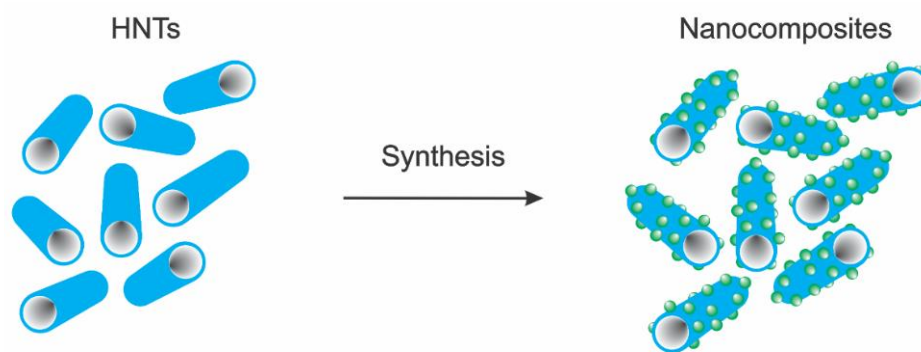


Figure 4. Schematic representation of halloysite-based nanocomposites.

Nanostructured nanocomposites were obtained from organically modified microfibrillar sepiolite and TiO_2 anatase nanoparticles. The TiO_2 /sepiolite nanocomposites were used in photocatalytic tests with phenol molecule as the pollutant model [38]. The characterizations of the nanocomposites indicate the formation of anatase nanoparticles dispersed in the sepiolite microfibers. In addition, the materials obtained have exciting surface properties. The authors found about 90% conversion of phenol from the irradiation tests, proving that nanocomposites are efficient for use in environmental remediation.

Photoactive materials were obtained by depositing titanium and/or zirconium oxides in the palygorskite clay mineral support, and the discoloration of a reactive dye (Remazol Brilliant Blue R) under UV light was investigated. TiO₂ and ZrO₂ nanoparticles were continuously dispersed onto palygorskite microfibers, increasing the specific surface area of nanocomposites. The photocatalytic tests indicate that the materials obtained from palygorskite show promise for degrading dyes as model pollutants [13].

Palygorskite clay mineral and layered double hydroxide (LDH) have supported incorporating TiO₂ (anatase) to form nanocomposite catalysts. TiO₂ was incorporated into the supports by the sol–gel method. Heterostructured materials were used with yellow eosin dye (YE) [39]. The scheme (Figure 5) shows after TiO₂ incorporation, illustrating that the nanoparticles coated the structure of the supports well. The nanocomposite presents the characteristic morphology of each structure (Palygorskite and LDH), and the TiO₂ nanoparticles are homogeneously dispersed and stabilized in the suitable heterostructure. In photocatalytic tests, the material had a discoloration rate of up to 99.08%, where photo holes and hydroxyl groups are probably the main reactive species involved in the photodegradation process.

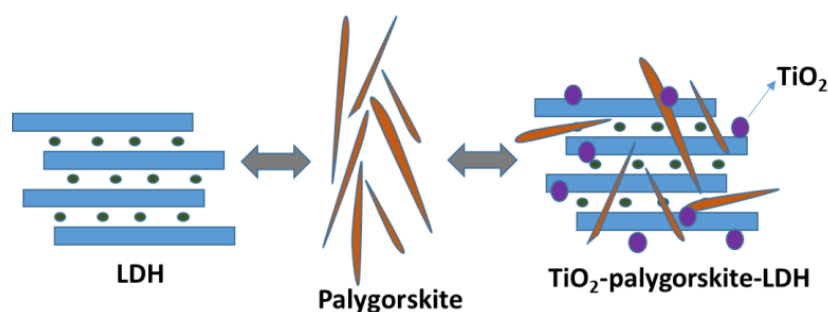


Figure 5. Representation of TiO₂-palygorskite-LDH nanocomposite formation by sol–gel route.

Some factors may limit the application of TiO₂, such as low quantum yield and high recombination rate of e⁻/h⁺ pairs. Other relevant characteristics can affect photocatalytic activity, such as shape and grain size, crystalline phase structure, and the presence of defects. Strategies are used to improve the stability and efficiency of semiconductors, such as doping or catalytic supports [40]. The stability of semiconductors is investigated with successive reaction cycles generally applied. When supported on clay minerals, these semiconductors have shown activity and stability after reuse, and no significant structural changes are observed in the materials. The results indicate that the effect of strong interactions between the nanoparticles and the support influences the excellent stability of semiconductors. Some examples of studies to investigate the stabilization of TiO₂ are [19,28,40].

4. Other Semiconductors Supported onto Different Clay Minerals

In addition to TiO₂, researchers have widely used other semiconductors. For example, bentonite was used to immobilize oxides of Nb₂O₅ (a semiconductor with abundant source in Brazil that shows low cost but is still rarely explored in photocatalytic studies). The obtained nanocomposite was investigated as a photocatalyst potential for removing reactive blue 19 dye in an aqueous medium [41]. Photocatalytic tests were performed in two forms: immobilized on glass slides and pellet form. The results indicated that the oxides were evenly immobilized onto the bentonite surface. Although both tests suggest high efficiency in the blue textile dye photodegradation, the nanoparticles synthesized in pellets showed a degradation rate of 98%, while in glass tests, the degradation rate was 78%.

Smectite supported with Fe₃O₄ nanoparticles was used to remove rhodamine B dye (RhB) from wastewater under UVA irradiation in studies by [42]. The nanocomposites showed high photocatalytic activity, degrading almost 100% of the dye in 25 min at pH 3. However, the nanocomposites also showed easy recoverability with the action of an external magnetic field.

In the studies by Guo et al. [43], the authors developed an Ag_3PO_4 /rectorite nanocomposite synthesized by the ultrasound-assisted method. The photocatalytic properties of the Ag_3PO_4 /rectorite were evaluated by decomposition of methylene blue dye under visible light irradiation. The nanocomposite photocatalyst synthesized via ultrasound techniques exhibits greatly enhanced photocatalytic performance in the degradation of methylene blue under visible light tests compared to pure Ag_3PO_4 [43].

Vermiculite was used to immobilize hematite nanoparticles to obtain stable photocatalysts [44], and $\alpha\text{-Fe}_2\text{O}_3$ nanoparticles/vermiculite clay mineral photocatalysts presented high activity for the CO_2 photocatalytic reduction. It is observed that vermiculites are not extensively studied in photocatalytic processes but have great potential.

As mentioned, ZnO has gained attention in environmental applications; these materials are considered more suitable mainly due to their high affinity for different pollutants, stability, and non-toxicity [45–47]. However, it is already known in the literature that nanoparticles agglomerate in solution and are challenging to recycle. In addition, depending on the application time, these materials can be deactivated. As a result, studies on the incorporation of semiconductor nanoparticles in stable matrices, such as clay minerals, have been increasing as a strategy to promote interfacial interactions, remedy the agglomeration and recoverability issues of the photocatalysts of the reaction medium [48].

ZnO/halloysite nanocomposites were obtained by seed-mediated growth method for methylene blue degradation. The ZnO/HNTs promoted the separation of electrons and holes in the ZnO surface and reduced the bandgap, thus improving the photocatalytic activity, enhancing the effective utilization rate of zinc oxide nanoparticles, and improving the separation of nanocomposite from the reaction medium [49].

Fe-doped ZnO nanoparticles were impregnated by co-precipitation method onto kaolinite clay mineral (ZnO/K), as used for visible light under photocatalytic disinfection (PCD) of *Enterobacter* sp Gram harmful bacteria. A comparative analysis was carried out with traditional disinfectants. Toxicity and reusability of the photocatalyst were also investigated [50]. The results showed complete disinfection of the bacteria using the nanocomposite ZnO/K irradiated under visible light. $\bullet\text{O}_2^-$ radicals were the reactive species responsible for bacterial cell damage. The kaolinite-based nanocomposite performed better than separate TiO_2 and ZnO semiconductors. In catalytic reactions, ZnO/K also appeared as a non-toxic and reusable material [50].

5. Routes of Synthesis and Influence of the Experimental Parameters

The synthesis of oxide–clay mineral structures can be carried out with the incorporation of previously obtained nanoparticles and the formation of nanoparticles during the synthesis of the nanocomposites (in situ preparation) [32]. The sol–gel method is the most commonly used to obtain photocatalysts based on oxides and clay minerals, but other methods are also found in the literature. The characteristics of the NPs on clay minerals vary depending on the preparation conditions. Some synthesis methods, synthesis parameters, and photocatalytic test parameters referring to different oxide–clay mineral photocatalysts are summarized in Table 1.

Table 1. Synthesis methods, reaction parameters, and application of the different photocatalysts.

Photocatalyst	Synthesis Method	Conditions of Photocatalytic Reaction	Pollutant	Ref.
TiO ₂ /montmorillonite	Solvothermal (190 °C/2 h)	Mercury lamp (500 W, ~365 nm), MB (1.0 × 10 ⁻⁴ , 100 mL), photocatalyst (50 mg)	Methylene blue (MB)	[51]
TiO ₂ /kaolinite	Impregnation method (500 °C/3 h)	Artificial solar light or UV-lamp (UV-A (365 nm), Black-Ray B 100 W UV-lamp, V-100AP series); RB19 (75 mg L ⁻¹ , 200 mL); photocatalyst (100 mg)	Reactive blue 19 (RB19)	[52]
TiO ₂ /Laponite	Hydrothermal (500 °C/12 h) (500 °C/3 h)	GHO436T5L type lamp irradiating in the UV-C region at 254 nm with 13 W UV-radiant and GHO245T6L/4-UVA type lamp irradiating in the 316–400 nm range with 4.6 W UV power; phenol (5 × 10 ⁻⁵ M), photocatalyst (0.1–0.4 g L ⁻¹)	Phenol or 2,4,6-trichloro phenol (TCP)	[53]
TiO ₂ /pyrophyllite	Sol-gel (450–850 °C/4 h)	UV illumination; phenol (50 mg. L ⁻¹ , 200 mL); photocatalyst (1.0 g L ⁻¹)	Phenol	[54]
Zr doped TiO ₂ /Cloisite	Sol-gel (500 °C/4 h)	765–250 W m ⁻² Xe lamp (61–24 W m ⁻² from 300 to 400 nm, 1.4 × 10 ²⁰ –5.5 × 10 ¹⁹ photons m ⁻² s ⁻¹); Antipyrine (10 mg L ⁻¹ , 200 mL); photocatalyst (250 mg L ⁻¹)	Antipyrine	[55]
W doped TiO ₂ /Cloisite	Sol-gel (500 °C/4 h)	Solar lamp (300 W Xenon lamp, Newport Corporation); Atrazine (2.5 mg L ⁻¹ , 10 mL); photocatalyst (0.25 g L ⁻¹)	Atrazine	[56]
TiO ₂ /sepiolite	Colloidal route (500 °C/6 h)	Hg arc lamp (150 W, 280–600 nm); phenol (0.5 mmol L ⁻¹ , 375 mL)	Phenol	[38]
ZnO/smectite	Colloidal route (500 °C/2 h) (500 °C/4 h)	300 W UV lamp (Osram Ultra Vitalux 240 V 300 W E27 UVA/UVB); ibuprofen (10 ppm, 100 mL); photocatalyst (25 mg)	Ibuprofen	[57]
ZnO/sepiolite	Colloidal route (500 °C/1 h) (500 °C/4 h)	Xe lamp and a Solar ID65 filter that cuts off the UV light contribution at 320 nm, fixing the irradiation intensity at 450 W m ⁻² ; target compound (10 mg L ⁻¹); photocatalyst (250 mg L ⁻¹)	Ibuprofen (IBU), acetaminophen (ACE) and antipyrine (ANT)	[58]
BiVO ₄ /palygorskite	Hydrothermal (400 °C/4 h)	500-W Xe lamp, 540 nm; TC (30 mg L ⁻¹ , 50 mL); photocatalyst (50 mg)	Tetracycline (TC)	[59]
Pd-CuO/palygorskite	Precipitation method (60 °C/4 h)	UV light (2 × 15 W UV tubes predominantly emitting at 365 nm); MO (25 ppm, 100 mL); photocatalyst (50 mg)	Methyl orange dye (MO)	[60]
Fe ₃ O ₄ /smectite	Precipitation method (50 °C/48 h)	UVA lamp (350 nm); RhB (100 mg L ⁻¹); photocatalyst (0.5–2 g L ⁻¹)	Rhodamine B (RhB)	[42]
Co ₃ O ₄ /halloysite	Ultrasonic-assisted method (50 °C/3 h)	UV radiation source was a 60 W high-pressure mercury lamp; MB (200 mg L ⁻¹ , 200 mL); photocatalyst (50 mg)	Methylene blue (MB)	[61]
g-C ₃ N ₄ /Na-bentonite	Ultrasonic-assisted method (550 °C/2 h)	350 W xenon lamp visible-light irradiation (λ > 420 nm); RhB (20 ppm, 100 mL) and/or Cr(VI) (50 ppm, 100 mL); photocatalyst (1 g L ⁻¹)	Rhodamine B (RhB) and hexavalent chromium (Cr(VI))	[62]
Bi ₂ NbO ₅ F/rectorite	Ultrasonic-assisted method (60 °C/24 h)	UV lamp (λ = 254 nm, 20 W, 0.524 mWcm ⁻²); RhB (5 mg L ⁻¹ , 100 mL); photocatalyst (0.1 g L ⁻¹)	Rhodamine B (RhB)	[63]
CdS/clay minerals	Hydrothermal (180 °C/6 h)	300 W xenon lamp (providing visible light ≥ 400 nm); CR (30 mg L ⁻¹ , 50 mL); photocatalyst (30 mg)	Congo red dye (CR)	[64]

Photocatalytic degradation is a reliable and promising water treatment technology to degrade organic dye pollutants. Semiconductor nanoparticles, mainly TiO₂, can be

loaded on some supports to improve dispersion and recovery. There is a wide variety of clay mineral structures, which consequently influence their characteristics and properties, expanding the loading possibilities of several semiconductors that can be incorporated in the internal or external surfaces of the supports. At the same time, there is a diversity of reserves of natural clay minerals with specific properties of cost and accessibility, where this step can also be decisive in the choice and applicability of these materials as catalytic supports [26]. From the different studies collected in the literature, the significant variation in the synthesis parameters of the photocatalysts was observed, and different substrates were highlighted at different initial concentrations. However, in the most varied studies, what is indisputable is the improvement of the photocatalytic activity of semiconductors when supported on clay minerals, even with different morphologies. See recent publications of these materials, including reviews [20,32,48,65] that address the clay minerals supported with oxides and applied in environmental decontamination.

Lopes et al. [66] prepared a TiO₂/kaolinite nanocomposite by sol–gel method aiming at the photocatalytic decomposition of Coomassie brilliant blue dye (CBB). They placed 10 g of kaolinite in contact with 200 mL of deionized water and kept it at 60 °C and under continuous stirring for four hours, at pH 4.54. The TiO₂ dispersion was obtained by the hydrolysis of 20 mL of titanium tetraisopropoxide precursor in a 0.5 mol L⁻¹ HCl solution. After a 4 h reaction, the TiO₂ solution was slowly added to the kaolinite dispersion under mechanical stirring. The solid was separated and dried at 100 °C for 24 h, divided into four portions, and calcined at different temperatures for two hours. The photocatalytic tests were performed in the presence of oxidizing agents and nanocomposite in dye decolorization and were studied using pure kaolinite and commercial TiO₂. Commercial TiO₂ has a higher rate of dye degradation than the nanocomposite synthesized at 300 °C, and this result implies a higher mass ratio of commercial TiO₂ compared to the mass present in the nanocomposite. Figure 6 demonstrates that the TiO₂/kaolinite nanocomposite increases the CBB dye solution photodegradation. From the photocatalytic tests, the nanocomposites showed high activity, and the best performance was obtained when the material was calcined at 300 °C and a concentration of 1.5 g L⁻¹. The high activity was due to pre-adsorption of the pollutant on the nanocomposite surface due to their convenient specific surface area and porosity [66].

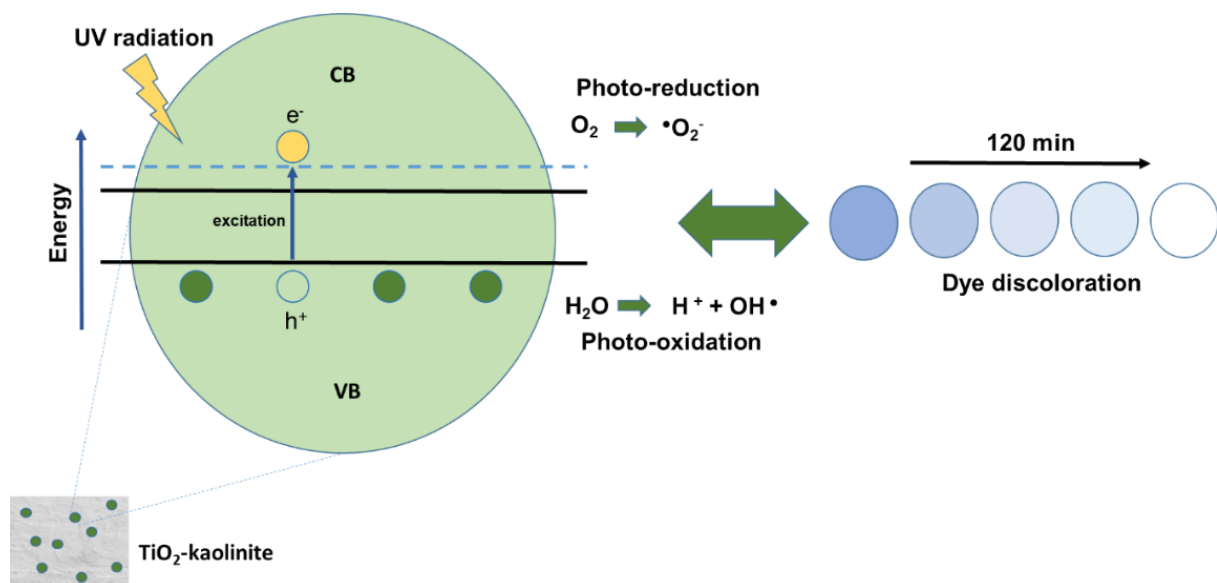


Figure 6. Photocatalysis mechanism proposal for discoloration of the blue dye solution from kaolinite-based nanocomposite under UV light.

Studies by [37] describe the synthesis of TiO₂ nanoparticles supported on sepiolite (Sep) and halloysite (Hal) using the hydrothermal method under low temperatures and without stabilizing agents. TiO₂ sol was obtained by hydrolysis of titanium tetraisopropoxide in hydrochloric acid, water, and ethanol. First, the TiO₂ sol was added to clay mineral dispersion (1% w/w), where the clay mineral: TiO₂ ratio was 30:70. Next, the slurry was stirred for 24 h, and the resulting dispersion was centrifuged for 10 min followed by three centrifuge items of washing. The TiO₂/clay mineral nanocomposite was then dispersed in water: ethanol solution (1:1 ratio) to hydrothermal treatment in an autoclave reactor for 5 h at 180 °C. Finally, the solid was separated by centrifugation and oven-dried for 3 h at 60 °C. This study performed photocatalytic tests to degrade paracetamol, tetracycline, and rhodamine B (RhB). The photodecomposition of the different compounds was investigated under UV-visible light irradiation and compared to that of commercial titanium dioxide (P25). The TiO₂/Sep nanocomposite presented the highest activity of all three nanocomposites. However, the photocatalytic activity of all nanocomposites in decomposing both RhB and tetracycline is higher than P25. Through the analysis of total organic carbon (TOC), the decomposition and mineralization of paracetamol and tetracycline were monitored during the photodegradation process using the TiO₂/Sep nanocomposite, chosen because it presented the best activity.

ZnO/kaolinite nanocomposite was used in the photocatalytic degradation of the 2-chlorophenol (2-CP) contaminant in water [67]. For the preparation of nanocomposites, 10 g of clay mineral was first dispersed in 250 mL of 0.9 M NaOH solution. The mixture was stirred at 55 °C. Separately, a zinc acetate solution (250 mL, 0.68 M) was prepared and added dropwise to the clay mineral dispersion. The ZnO/kaolinite precipitate was recovered and washed with distilled water several times until achieving neutral pH. The solid was dried and calcined to 450 °C for 1 h. Different preparations were made without ZnO in the synthesis for control and comparison. The clay mineral was treated under the same conditions without zinc oxide nanoparticles. Photocatalytic experiments were performed using naked ZnO, treated clay mineral, and ZnO/kaolinite nanocomposite exposed to direct sunlight. The prepared nanocomposite exhibited superior 2-CP adsorption and photodegradation compared to ZnO nanoparticles. Comparing different media, at pH 8.7, maximum adsorption and maximum degradation of pollutant molecules were observed. In addition, the photocatalyst has excellent reusability and was quickly recovered from the reaction medium. Complete mineralization of 2-chlorophenol was verified [67].

Thermal and impregnation methods were used to obtain the Ag-loaded Bi₂O₃/montmorillonite functionalized nanocomposite [68]. The photocatalytic efficiency of the nanocomposite was investigated in the degradation under visible light of the tetracycline antibiotic (TC) and the rhodamine B dye (RhB). The mineralization potential of the pollutant compounds and other operational factors, such as pH, pollutant concentration, and photocatalyst concentration, were evaluated. In addition, the impact of Ag nanoparticles in the photocatalytic process and the investigation of the nanocomposite stability were considered. The synthesized Bi₂O₃/Mt using 1 g of the clay mineral was dispersed in 75 mL of water and ultrasonicated for 1 h. Separately, 1.5 mmol of Bi(NO₃)₃·5H₂O was dissolved in 20 mL of a 1 M nitric acid solution. The precursor solution was added to the clay mineral dispersion and maintained under stirring for 2 h, at pH 11. The precipitate was recovered, dried at 70 °C for 6 h, and calcined at 400 °C for 3 h. The impregnation method was used for Ag incorporation and to obtain the Ag@Bi₂O₃/Mt nanocomposite, where 50 mL of an AgNO₃ solution was added to a solution of ascorbic acid and dripped NaOH, kept under stirring for 1 h. Then, 500 mg of Bi₂O₃/Mt was dispersed in 10 mL of ethanol and stirred for 2 h. The solid was washed and dried at 70 °C for 6 h. The photocatalytic efficiency becomes remarkably amplified after incorporating Ag NPs on Bi₂O₃/Mt nanocomposite [68]. In this study, the combination of the Bi₂O₃ nanoparticles, the presence of Ag, and the support selected to improve the surface area, the adsorption, and the efficiency photo responsible in the visible region were used. The bandgap and charge separation favors the photocatalytic

activity of the nanocomposite. The formation of the montmorillonite-based nanocomposite also highlighted the stability and recovery of the photocatalyst.

Based on the literature, TiO_2 and ZnO are the most applied semiconductors in photocatalysis studies in the environmental field, but recently several other photocatalysts have been demonstrated as efficient. The search for new materials with stability, low cost, reusability, and the possibility to obtain on a large scale for industrial applications has increased the number of studies involving new catalysts supported on clay minerals. The research shows the versatility of the clay minerals used as a support to obtain different nanocomposites applied efficiently in the photocatalytic processes of different polluting organic compounds. In addition, the development of materials allows the design of clay mineral-based composites that combine the adsorptive and photocatalytic ranges.

6. Pillared Clay Minerals for Photodegradation Process

Pillared clay minerals are extensively studied among several porous materials developed by molecular science and engineering. These solids, also known as reticulated clay minerals or clay minerals interlayered with pillars (PILCs), are obtained by ionic exchange of cations present in the interlayer space, with inorganic polycations calcination required to form the oxide pillars [69,70]. After the intercalation reaction of the polyhydroxycation clusters, the interlayer spacing of the clay is increased. The heat treatment forms the structures called oxide pillars without destroying the ordering of the clay mineral layers. The pillarization process involves the formation of permanent porosity, new active surfaces and promotes a chemically stable structure. Different synthesis methods can be used to prepare these materials, expanding their field of application [70]. Al cluster cation is the most used precursor, but other Ti- or Zr-based oligomers, for example, have also been studied. Two main steps are followed for pillarization with these compounds, as mentioned. First is the intercalation of the polycations. The second step, calcination, results in an essential characteristic of PILCs: increasing interbasal distance. The increase in porosity, accessibility, and acidity are consequences of this process of chemical modification of the supports. Stable links between the formed pillars and the clay mineral surface are proposed and discussed to explain the high stability of these structures [71]. Thus, pillared clay minerals with larger pore size and thermal stability have frequently been used as catalysts or support for catalytic reactions [72].

PILCs are constantly used to remove hazardous substances in an aqueous medium as catalysts support other active catalytic phases. Titanium-pillared clay minerals are extensively studied for photodegradation of contaminants, and this material may have an activity superior to TiO_2 nanoparticles [73]. Figure 7 presents the general synthesis scheme for the preparation of pillared clay minerals.

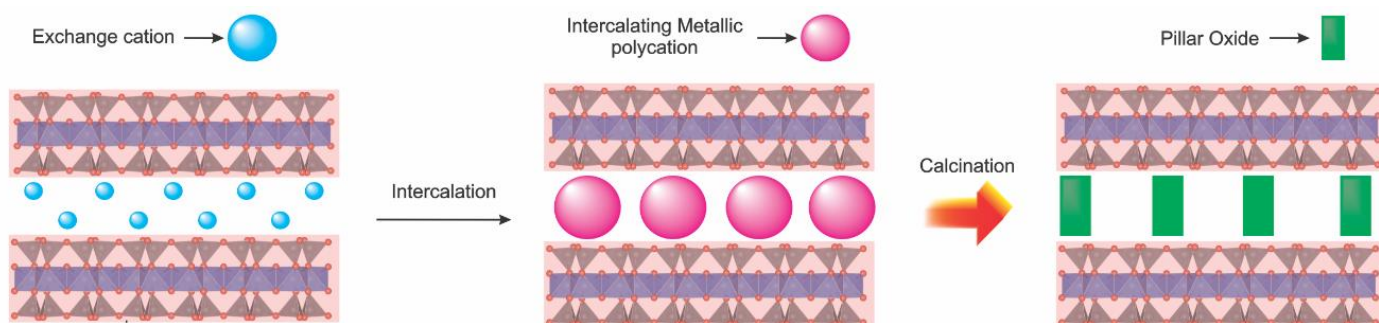


Figure 7. Schematic representation of the pillarization process of clay minerals.

Mica modified with Mg or Fe was used to obtain pillared clay mineral with TiO_2 in the studies of [74]. The photodecomposition tests used methyl orange (MO) as a model pollutant. The pillared clay minerals exhibited a surface area much higher than the raw

materials. Photocatalytic properties of TiO₂/pillared mica are significantly influenced by the specific surface area and optical transparency of host clay mineral layers [74].

In [75], the authors developed a photocatalyst based on pillared clay minerals with titanium oxide. First, the TiO₂/clay mineral nanocomposites were immobilized by the sol–gel method in organic/clay mineral-exchanged with the cationic surfactant cetyltrimethylammonium bromide (CTMABr). Then, titanium pillared clay mineral was applied in pesticide photodegradation. In this case, TiO₂ based nanomaterial showed high photocatalytic activity in the degradation of 2,4-dichlorophenoxyacetic acid and 2,4-dichlorophenoxypropanoic acid pesticides.

TiO₂ and Fe doped TiO₂/pillared bentonite clay were used to photodegrade the toxic microcystin-LR under UV light irradiation and in the presence of an oxidizing agent. According to [76], microcystin-LR contains a lot of amine functional groups, which will readily be adsorbed onto TiO₂/PILCs due to superficial acidity. Nevertheless, the target molecules are significant enough to be inserted in the pillared matrix. Fe and H₂O₂ have solid oxidizing properties, and during photocatalysis, they can produce reactive species that degrade microcystin-LR molecules. In this case, the proposed mechanism is that the microcystin-LR molecules are first broken down into smaller organic molecules on the surface of the photocatalyst by the action of Fe-doped TiO₂/PILCs nanocomposite. The large microcystin-LR molecules were mainly converted into smaller molecules of hydrocarbons, carboxylic acids, and organic amines through Fenton-type oxidation in the presence of H₂O₂. After the reaction, the smaller intermediate molecules can diffuse and settle between the TiO₂ pillars, and thus be mineralized by the catalytic action of the TiO₂ pillars. In this case, complete mineralization was not observed, probably due to the deactivation of the photocatalyst [76].

Bachir et al. [77] prepared the TiO₂/Mt and Pd-TiO₂/Mt pillared photocatalysts using the sol–gel method and microwave calcination. The prepared materials were tested to evaluate their potential for removing phenyl urea herbicide (Linuron) from aqueous solutions by adsorption and photodegradation methods. The XRD diffractograms indicate the success of the pillarization process and the absence of peaks corresponding to the phase containing palladium in the doped samples, suggesting the incorporation of Pd in the lattice of TiO₂ pillars. The textural analysis shows the high porosity of the nanocomposites. The higher surface area for the pillared undoped and Pd-doped materials indicates the volume of pores in these two samples, more significant than in the pristine one. The thermogravimetric analysis indicates high thermal stability [77]. The photosensitive and doped materials showed significant photocatalytic activity under visible light for herbicide decomposition.

Pillared montmorillonite undoped and Cr³⁺ or Fe³⁺ doped titanium oxides were prepared and used in photocatalytic degradation of trimethoprim antibiotics in an aqueous solution under UV irradiation [78]. Cr³⁺ doped clay mineral displayed superior properties, with close to 76% photodecomposition after 180 min of reaction. The photodegradation mechanism was investigated by mass spectrometry. The general procedure seemed to be the breakage of fragments in the TMBz (3,3',5,5'-tetramethylbenzidine) intermediate of the molecule, with the further reaction of these fragments with its molecule, mainly with the very reactive methoxy groups, leading to species more significant than the initial molecule, followed by further degradation steps [78].

Catalytic wet peroxide oxidation (CWPO) has become an exciting alternative for application in environmental remediation. This strategy can replace the Fenton-like process when Fe is incorporated into the surface of materials, such as clay minerals [79]. Natural clay minerals can stand out as supports for semiconductors for photodegradation of organic contaminants by the CWPO process. For example, Fe-Co/pillared clay mineral photocatalyst was prepared for paracetamol (PCM) drug degradation. Among pharmaceutical compounds that can pollute water, paracetamol deserves particular attention since it has recently been discovered as a potential pollutant of waters. The presence of iron and cobalt ions proves the photocatalytic action of metals present in pillared clay minerals since the acidic and textural analyses of the functionalized samples are very similar to

the starting materials. Moreover, it shows the participation of the active phases in the photodegradation of paracetamol. In this case, where the Fe ions are probably anchored in the cobalt pillars, the leaching of the iron was not significant, which indicates the efficiency of the nanocomposite in the drug removal process [79].

Pillared montmorillonite (Al/Mt) and FeAl/Mt were investigated as hydroxyl-metal pillared Mt to load Ag_3PO_4 . New photocatalysts ($\text{Ag}_3\text{PO}_4/\text{Al}/\text{Mt}$ and $\text{Ag}_3\text{PO}_4/\text{FeAl}/\text{Mt}$) were obtained, and their potential activity was tested in the oxidative degradation of acid red 18 dye (AR18) [80]. The photocatalysis and stability tests showed a better behavior for the $\text{Ag}_3\text{PO}_4/\text{FeAl}/\text{Mt}$ nanocomposite. In addition, the nanoparticles of Ag_3PO_4 would be more evenly dispersed on the surface of the pillared support, promoting the separation of charges and increasing the activity under visible irradiation.

Raw bentonite was used to support the preparation of photocatalysts based on single and mixed pillars. The photocatalysts (Al/PILCs, Zr/PILCs, and Al-Zr/PILCs) were obtained by the microwave-assisted method and applied to the decomposition of phenol by catalytic wet air oxidation (CWAO) [81]. CWAO is considered a promising technology among the advanced oxidation processes in the application of water decontamination. The authors concluded that the ultrasonic method reduces the synthesis time compared to traditional pillarization synthesis methods. In addition, the results indicated greater specific surface area and pore volume, more excellent thermal stability, and surface acidity for the mixed pillared nanocomposite when compared with materials with single pillar and pure bentonite. Therefore, it can be concluded that Al-Zr/PILCs have exciting characteristics to be applied in removing phenol by the CWAO process under mild conditions [81].

Pillared clay minerals are prominent photocatalysts mainly due to the accessibility of targeted organic pollutants that diffuse to the active sites of the pillars present in the interlamellar spaces [8]. Advances in the preparation, characterization, and applications of pillared clay minerals have been comprehensively studied in several works, and the progress in investigations in materials synthesized by different techniques can obtain photocatalysts that are different from those based on TiO_2 . Clay minerals pillared with aluminum, mixed pillars, and doped materials, have gained space in photocatalytic studies to degrade various pollutants, such as dyes, drugs, pharmaceuticals, herbicides, or pesticides.

7. Advantages and Disadvantages of Photocatalysts Supported on Clay Minerals

Therefore, the literature widely reports that different structures can be obtained by different routes and applied to heterogeneous photocatalysis in the environmental field. Some authors cite the advantages (or disadvantages) of using clay minerals to support semiconductors and form highly efficient catalysts.

Some advantages (low cost, high availability, high mechanical and/or thermal stability, modification of its physicochemical properties) and disadvantages (irreproducibility since the mineral deposits on the Earth are different, clay mineral has anisotropic properties) can be cited.

Thus, clay minerals used as support permits the iron-based magnetic nanoparticles' surface area to increase by providing a matrix facilitating dispersion [42]. Thus, the resulting magnetic nanoparticles have more beneficial properties, such as lesser co-aggregation, smaller particle sizes, and higher thermal and chemical stability than those without support materials.

For [60], the support-based photocatalysts, which can adsorb and concentrate the reactants, still allow the latter to diffuse from the adsorption site to the photocatalyst surface, and were quite efficient in improving the degradation rate of pollutants.

The overall efficiency of the catalyst can decrease when supported, as the illuminated surface decreases considerably. Thus, porous materials with a high specific surface area, such as silica, zeolites, activated carbon, or clay minerals, are alternative materials explained from studies of [82].

In their conclusion, the authors elucidate the application of pillared clay minerals in the environmental field but report that a better approach is still needed on some issues, such

as the cost of pillaring agents that modify the clay minerals, better evidence for removing pharmaceutical wastewater, and the applicability of pillar clay minerals for removing VOCs [72].

Akkari et al. [58] investigated different incorporating metallic nanoparticles and functionalizing clay minerals to obtain interesting heterostructures for photocatalytic properties. In their studies, the authors highlight the use of clay minerals to support the incorporation of TiO₂ and ZnO nanoparticles obtained by different routes. The sepiolite-based heterostructures have especially relevant results in removing drugs in solution. Moreover, the new approaches lead to highly efficient and relatively inexpensive photocatalysts.

Additionally, TiO₂ nanoparticles have been one of the most popular photocatalysts in practical applications [26]. However, two main problems are reported in the use of TiO₂ for wastewater decontamination. One of them is the aggregation of nanoparticles (with high Gibbs free energy) that can cause the deactivation of the photocatalyst. The other is the difficulty of recovering the photocatalyst from the reaction medium. Therefore, the authors highlighted the incorporation of nanoparticles to reduce agglomeration and facilitate their recovery. Several supports can be used, such as silica, zeolites, graphene, activated carbon, and clay minerals. This last one stands out for its ample reserve, availability, distribution, and relatively low cost.

In another study, Akkari et al. [83] used hybrid ZnO/organoclays to develop different heterostructures that might introduce several functionalities controlled by the coverage of the clay mineral backbone by the selected NPs of metallic oxide. Those authors stated the need to increase the number of porous heterostructures functionalized with clay minerals to prepare efficient catalysts for industrial applications.

In the studies of [84], TiO₂ is the most widely used semiconductor. However, the recovery of ultrafine nanoparticles from water is tricky, resulting in difficulties in separation, recovery, and reuse, and the TiO₂ nanoparticle clusters are unfavorable to the photocatalytic property. Therefore, research has focused on developing new TiO₂ photocatalysts loaded on different supports. Those authors stated that pillared clay minerals have high photocatalytic activity, but with some structural problems, such as limited light to diffuse to the internal anatase sites between the layers to initiate the reaction, small particles, and difficulty in degrading large molecules of organic compounds. Therefore, the use of clay minerals with a fibrous structure has become a viable and promising alternative for obtaining new photocatalysts.

For [68], the development of an efficient catalyst in a broader region of the spectrum promoting charge separation, obtained through the combination of a natural substrate with metallic nanoparticles, can be promising in the field of water decontamination. In Mt and Bi₂O₃/Mt nanocomposites, Ag acts as an inhibitor of electron/hole pair recombination due to Ag NPs surface plasmon resonance (SPR). The montmorillonite-based nanocomposites showed a high specific surface area and promoted the formation of more active sites and facilitated the recoverability of the Ag@Bi₂O₃/Mt suspended photocatalyst. Figure 8 illustrates the schematic representation of the electron-hole separation of oxide-clay mineral nanocomposite and photocatalysis method under visible light irradiation for organic compounds degradation.

New-found investigations have demonstrated the effectiveness of combining adsorption and photocatalysis properties in studies involving the incorporation of semiconductors in the structure of clay minerals [85,86]. For example, Lazaar et al. [87] demonstrated a significant increase in discoloration of the methylene blue when using adsorption and the photocatalysis process, reaching a dye removal of up to 98% after 300 min of reaction using TiO₂/natural clay mineral nanocomposites. Chkirida et al. [88] also demonstrated the effect of the adsorption and photocatalysis properties of TiO₂/alginate/bentonite biocomposites for the degradation of methylene blue dye. The authors observed that integrating adsorption and photocatalysis features achieved up to 96% of removal of the dye in aqueous media, a superior result when applied to the adsorption and photocatalysis processes separately.

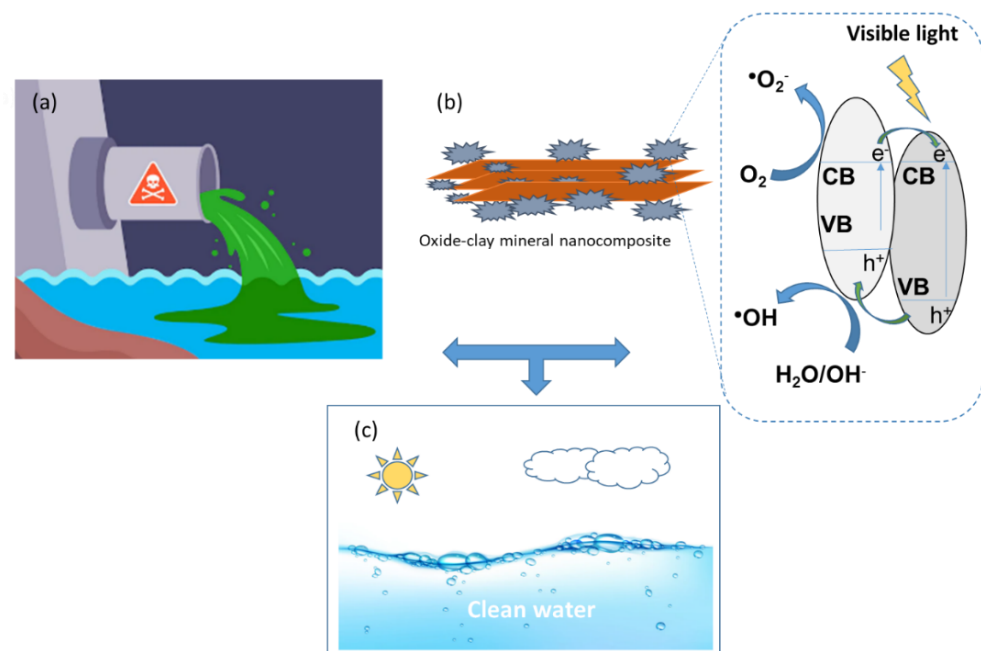


Figure 8. Representative scheme in sequence of the (a) polluted wastewater, (b) oxide–clay mineral nanocomposite reaction mechanism in the photocatalytic degradation of organic compounds and (c) clean water after treatment.

Even as clay minerals, other supports are investigated, mainly due to their high surface area and robust and stable structures, and some features. We can observe some interesting facts from the efficiency of semiconductors supported in materials other than clay minerals. For example, the TiO_2 -zeolite photocatalysts in the studies by [89] showed a greater discoloration rate of methyl orange dye under UV light after doping with Pt. In [90], studies supported nano titanium dioxide prepared using mesoporous silica materials. The mean pore of silica support and the mean titania particle size plays an essential role in the photoactivity shown by the materials prepared. Using an active carbon (AC) in this investigation, [91] synthesized TiO_2 -activated carbon composite (TiO_2/AC) and applied it to the decomposition of tetracycline (TC), a lower bandgap was observed in the composite and high photodegradation rates were achieved. For [92], the Fe-based metal–organic frameworks (MOFs) showed simultaneous adsorption and photodegradation efficiency in removing tetracycline in solution.

8. Future Perspectives

From the various studies that report the use of supported or pillared clay minerals with different semiconductors, numerous advantages are presented in the synthesis process of new clay mineral-based materials and the applicability in photocatalytic studies. It is possible to highlight some characteristics of the systems, mainly about the stability of the obtained materials, low cost, reusability, and recovering the photocatalyst from the reaction system. In the supporting materials, photocatalytic activity improvement occurs mainly when the results are compared by per mass of pure semiconductors. Different routes can obtain several structures and efficiently be applied in the photocatalytic degradation of different hazardous contaminants.

The search for new efficient, ecologically correct, and recoverable materials is an incentive for new approaches to syntheses and new semiconductors supported in clay minerals. The new features of these materials may be required for use under irradiation of sunlight, which is a clean, accessible, and renewable energy source. In this sense, new semiconductors that achieve maximum efficiency in a broad light absorption spectral range can be a challenge.

With the use of clay minerals as a support, a consequence may be better diffusion of the adsorbed emerging contaminants, followed by the transfer of the interphase to the supported semiconductor, where the synergistic effect between the semiconductor nanoparticles and the structure of the clay mineral matrix can occur, contributing to a complete photodecomposition pathway. In addition, the adsorption capacity of the matrices potentially improves the removal of the pollutant in aqueous media.

Therefore, clay minerals are suitable supports for developing advanced materials that can be used in water decontamination by photochemical processes or extended to new functionalities, strongly contributing to studies in the field of environmental remediation.

9. Conclusion Remarks

In this work, several studies were gathered about the application of clay minerals as catalytic supports for photocatalysis processes. Different synthesis routes have been developed as new strategies for immobilizing metallic semiconductors in the structure of different clay minerals, whether with lamellar, tubular, or fibrous morphology. The clay minerals have colloidal properties and surface chemistry propitious to photocatalysis, facilitating the reaction process. The increase in surface area and adsorption capacity, the homogeneous distribution of nanoparticles, the reduction of agglomerates, charge separation, stability, reusability, and recovery of photocatalysts, may be the advantages of using clay minerals as support for obtaining these new functional materials to remove manifold emerging contaminants through photodegradation.

Author Contributions: All authors contributed to the study conception and design. W.F.: methodology, writing—original draft; P.T.: conceptualization, visualization, writing—review and editing; T.M.: methodology; L.M.H.: methodology; E.C.S.-F.: visualization and writing—review; M.B.F.: supervision, conceptualization; J.A.C.: writing—review and editing; J.O.: supervision, conceptualization, project administration, writing—review and editing; and M.G.F.: visualization and writing—review. All authors have read and agreed to the published version of the manuscript.

Funding: This research was funded by Capes and Cnpq agencies.

Institutional Review Board Statement: Not applicable.

Informed Consent Statement: Not applicable.

Data Availability Statement: Not applicable.

Acknowledgments: The authors thank the Capes and Cnpq Agencies, UFPI, UFMA, UFPB and UMA institutes.

Conflicts of Interest: The authors declare no conflict of interest.

References

1. Khan, S.; Naushad, M.; Govarthan, M.; Iqbal, J.; Alfadul, S.M. Emerging contaminants of high concern for the environment: Current trends and future research. *Environ. Res.* **2022**, *207*, 112609. [[CrossRef](#)] [[PubMed](#)]
2. Rodriguez Narvaez, O.M.; Peralta-Hernandez, J.M.; Goonetilleke, A.; Bandala, E.R. Treatment technologies for emerging contaminants in water: A review. *Chem. Eng. J.* **2017**, *323*, 361–380. [[CrossRef](#)]
3. Taheran, M.; Naghdi, M.; Brar, S.K.; Verma, M.; Surampalli, R.Y. Emerging contaminants: Here today, there tomorrow! *Environ. Nanotechnol. Monit. Manag.* **2018**, *10*, 122–126. [[CrossRef](#)]
4. Andreozzi, R.; Caprio, V.; Insola, A.; Marotta, R. Advanced oxidation processes (AOP) for water purification and recovery. *Catal. Today* **1999**, *53*, 51–59. [[CrossRef](#)]
5. Cuerda-Correa, E.M.; Alexandre-Franco, M.F.; Fernández-González, C. Advanced Oxidation Processes for the Removal of Antibiotics from Water. An Overview. *Water* **2020**, *12*, 102. [[CrossRef](#)]
6. Herrmann, J.-M. Heterogeneous photocatalysis: Fundamentals and applications to the removal of various types of aqueous pollutants. *Catal. Today* **1999**, *53*, 115–129. [[CrossRef](#)]
7. Honorio, L.M.C.; De Oliveira, A.L.M.; Filho, E.C.D.S.; Osajima, J.A.; Hakki, A.; Macphee, D.E.; Dos Santos, I.M.G. Supporting the photocatalysts on ZrO₂: An effective way to enhance the photocatalytic activity of SrSnO₃. *Appl. Surf. Sci.* **2020**, *528*, 146991. [[CrossRef](#)]
8. Szczepanik, B. Photocatalytic Degradation of Organic Contaminants over Clay-TiO₂ Nanocomposites: A Review. *Appl. Clay Sci.* **2017**, *141*, 227–239. [[CrossRef](#)]

9. Alamdari, S.; Ghamsari, M.S.; Afarideh, H.; Mohammadi, A.; Geranmayeh, S.; Tafreshi, M.J.; Ehsani, M.H.; Ara, M.H.M. Preparation and characterization of GO-ZnO nanocomposite for UV detection application. *Opt. Mater.* **2019**, *92*, 243–250. [[CrossRef](#)]
10. Sun, S.; Zhao, R.; Xie, Y.; Liu, Y. Photocatalytic degradation of aflatoxin B1 by activated carbon supported TiO₂ catalyst. *Food Control* **2019**, *100*, 183–188. [[CrossRef](#)]
11. Li, Y.; Zhao, H.; Yang, M. TiO₂ nanoparticles supported on PMMA nanofibers for photocatalytic degradation of methyl orange. *J. Colloid Interface Sci.* **2017**, *508*, 500–507. [[CrossRef](#)] [[PubMed](#)]
12. De Oliveira, W.V.; Morais, A.S.; Honorio, L.; Trigueiro, P.; Almeida, L.; Garcia, R.R.P.; Viana, B.; Furtini, M.B.; Silva-Filho, E.C.; Osajima, J.A. TiO₂ Immobilized on Fibrous Clay as Strategies to Photocatalytic Activity. *Mater. Res.* **2020**, *23*, 1–10. [[CrossRef](#)]
13. Miranda, M.O.; Viana, B.C.; Honório, L.M.; Trigueiro, P.; Fonseca, M.G.; Franco, F.; Osajima, J.A.; Silva-Filho, E.C. Oxide-Clay Mineral as Photoactive Material for Dye Discoloration. *Minerals* **2020**, *10*, 132. [[CrossRef](#)]
14. Bergaya, F.; Jaber, M.; Lambert, J. *Environmental Silicate Nano-Biocomposites*; Green Energy and Technology; Avérous, L., Pollet, E., Eds.; Springer: London, UK, 2012; Volume 50, ISBN 978-1-4471-4101-3.
15. Cecilia, J.A.; García-Sancho, C.; Vilarrasa-García, E.; Jiménez-Jiménez, J.; Rodríguez-Castellón, E. Synthesis, Characterization, Uses and Applications of Porous Clays Heterostructures: A Review. *Chem. Rec.* **2018**, *18*, 1085–1104. [[CrossRef](#)]
16. Bergaya, F.; Lagaly, G. *Chapter 1 General Introduction: Clays, Clay Minerals, and Clay Science*, 2nd ed.; Elsevier: Amsterdam, The Netherlands, 2006; Volume 1.
17. Santos, S.S.; França, D.B.; Castellano, L.R.; Trigueiro, P.; Filho, E.C.S.; Santos, I.M.; Fonseca, M.G. Novel modified bentonites applied to the removal of an anionic azo-dye from aqueous solution. *Colloids Surf. A Physicochem. Eng. Asp.* **2019**, *585*, 124152. [[CrossRef](#)]
18. Santos, S.S.; Pereira, M.B.; Almeida, R.K.; Souza, A.G.; Fonseca, M.G.; Jaber, M. Silylation of leached-vermiculites following reaction with imidazole and copper sorption behavior. *J. Hazard. Mater.* **2016**, *306*, 406–418. [[CrossRef](#)]
19. Li, X.; Peng, K.; Chen, H.; Wang, Z. TiO₂ nanoparticles assembled on kaolinites with different morphologies for efficient photocatalytic performance. *Sci. Rep.* **2018**, *8*, 11663. [[CrossRef](#)]
20. Papoulis, D. Halloysite based nanocomposites and photocatalysis: A Review. *Appl. Clay Sci.* **2018**, *168*, 164–174. [[CrossRef](#)]
21. Prasad, C.; Tang, H.; Liu, Q.Q.; Zulfiqar, S.; Shah, S.; Bahadur, I. An overview of semiconductors/layered double hydroxides composites: Properties, synthesis, photocatalytic and photoelectrochemical applications. *J. Mol. Liq.* **2019**, *289*, 111114. [[CrossRef](#)]
22. da Rocha, M.C.; Braz, E.M.D.A.; Honório, L.M.C.; Trigueiro, P.; Fonseca, M.G.; Silva-Filho, E.C.; Carrasco, S.M.; Polo, M.S.; Iborra, C.V.; Osajima, J.A. Understanding the effect of UV light in systems containing clay minerals and tetracycline. *Appl. Clay Sci.* **2019**, *183*, 105311. [[CrossRef](#)]
23. Pardo, L.; Domínguez-Maqueda, M.; Cecilia, J.A.; Rodríguez, M.P.; Osajima, J.; Moriñigo, M.; Franco, F. Adsorption of Salmonella in Clay Minerals and Clay-Based Materials. *Minerals* **2020**, *10*, 130. [[CrossRef](#)]
24. Ruiz-Hitzky, E.; Aranda, P.; Darder, M.; Rytwo, G. Hybrid materials based on clays for environmental and biomedical applications. *J. Mater. Chem.* **2010**, *20*, 9306–9321. [[CrossRef](#)]
25. Gu, S.; Kang, X.; Wang, L.; Lichtfouse, E.; Wang, C. Clay mineral adsorbents for heavy metal removal from wastewater: A review. *Environ. Chem. Lett.* **2019**, *17*, 629–654. [[CrossRef](#)]
26. Wu, A.; Wang, D.; Wei, C.; Zhang, X.; Liu, Z.; Feng, P.; Ou, X.; Qiang, Y.; Garcia, H.; Niu, J. A comparative photocatalytic study of TiO₂ loaded on three natural clays with different morphologies. *Appl. Clay Sci.* **2019**, *183*, 105352. [[CrossRef](#)]
27. Bello, M.M.; Raman, A.A.A. Synergy of adsorption and advanced oxidation processes in recalcitrant wastewater treatment. *Environ. Chem. Lett.* **2019**, *17*, 1125–1142. [[CrossRef](#)]
28. Osajima, J.A.; Sá, A.S.; Honorio, L.M.C.; Trigueiro, P.; Pinto, L.I.F.; Oliveira, J.A.; Furtini, M.B.; Bezerra, R.D.S.; Alcantara, A.C.S.; Silva-Filho, E.C. Au@Ag bimetallic nanoparticles deposited on palygorskite in the presence of TiO₂ for enhanced photodegradation activity through synergistic effect. *Environ. Sci. Pollut. Res.* **2021**, *28*, 23995–24007. [[CrossRef](#)]
29. Gomes, J.; Lincho, J.; Domingues, E.; Quinta-Ferreira, R.M.; Martins, R.C. N-TiO₂ Photocatalysts: A Review of Their Characteristics and Capacity for Emerging Contaminants Removal. *Water* **2019**, *11*, 373. [[CrossRef](#)]
30. Ibhaddon, A.O.; Fitzpatrick, P. Heterogeneous Photocatalysis: Recent Advances and Applications. *Catalysts* **2013**, *3*, 189–218. [[CrossRef](#)]
31. Li, J.; Wu, N. Semiconductor-based photocatalysts and photoelectrochemical cells for solar fuel generation: A review. *Catal. Sci. Technol.* **2014**, *5*, 1360–1384. [[CrossRef](#)]
32. Ruiz-Hitzky, E.; Aranda, P.; Akkari, M.; Khaorapapong, N.; Ogawa, M. Photoactive nanoarchitectures based on clays incorporating TiO₂ and ZnO nanoparticles. *Beilstein J. Nanotechnol.* **2019**, *10*, 1140–1156. [[CrossRef](#)]
33. Kibanova, D.; Trejo, M.; Destailats, H.; Cervinisilva, J. Synthesis of hectorite-TiO₂ and kaolinite-TiO₂ nanocomposites with photocatalytic activity for the degradation of model air pollutants. *Appl. Clay Sci.* **2009**, *42*, 563–568. [[CrossRef](#)]
34. Manova, E.; Aranda, P.; Martín-Luengo, M.A.; Letaïef, S.; Ruiz-Hitzky, E. New titania-clay nanostructured porous materials. *Microporous Mesoporous Mater.* **2010**, *131*, 252–260. [[CrossRef](#)]
35. Paul, B.; Martens, W.; Frost, R.L. Immobilised anatase on clay mineral particles as a photocatalyst for herbicides degradation. *Appl. Clay Sci.* **2012**, *57*, 49–54. [[CrossRef](#)]

36. Papoulis, D.; Komarneni, S.; Nikolopoulou, A.; Tsolis-Katagas, P.; Panagiotaras, D.; Kacandes, H.; Zhang, P.; Yin, S.; Sato, T.; Katsuki, H. Palygorskite- and Halloysite-TiO₂ nanocomposites: Synthesis and photocatalytic activity. *Appl. Clay Sci.* **2010**, *50*, 118–124. [[CrossRef](#)]
37. Papoulis, D.; Panagiotaras, D.; Tsigrou, P.; Christoforidis, K.; Petit, C.; Apostolopoulou, A.; Stathatos, E.; Komarneni, S.; Koukouvelas, I. Halloysite and sepiolite—TiO₂ nanocomposites: Synthesis characterization and photocatalytic activity in three aquatic wastes. *Mater. Sci. Semicond. Process.* **2018**, *85*, 1–8. [[CrossRef](#)]
38. Aranda, P.; Kun, R.; Martín-Luengo, M.A.; Letaïef, S.; Dékány, I.; Ruiz-Hitzky, E. Titania–Sepiolite Nanocomposites Prepared by a Surfactant Templating Colloidal Route. *Chem. Mater.* **2007**, *20*, 84–91. [[CrossRef](#)]
39. Morais, A.; Oliveira, W.V.; de Oliveira, V.V.; Honorio, L.M.; Araujo, F.P.; Bezerra, R.D.; Fechine, P.B.; Viana, B.C.; Furtini, M.B.; Silva-Filho, E.C.; et al. Semiconductor supported by palygorskite and layered double hydroxides clays to dye discoloration in solution by a photocatalytic process. *J. Environ. Chem. Eng.* **2019**, *7*, 103431. [[CrossRef](#)]
40. Alfred, M.; Omorogie, M.O.; Bodede, O.; Moodley, R.; Ogunlaja, A.; Adeyemi, O.G.; Günter, C.; Taubert, A.; Iermak, I.; Eckert, H.; et al. Solar-active clay-TiO₂ nanocomposites prepared via biomass assisted synthesis: Efficient removal of ampicillin, sulfamethoxazole and artemether from water. *Chem. Eng. J.* **2020**, *398*, 125544. [[CrossRef](#)]
41. Lacerda, E.H.C.; Monteiro, F.C.; Kloss, J.R.; Fujiwara, S.T. Bentonite clay modified with Nb₂O₅: An efficient and reused photocatalyst for the degradation of reactive textile dye. *J. Photochem. Photobiol. A Chem.* **2020**, *388*, 112084. [[CrossRef](#)]
42. Caglar, B.; Guner, E.K.; Keles, K.; Özdokur, K.V.; Cubuk, O.; Coldur, F.; Caglar, S.; Topcu, C.; Tabak, A. Fe₃O₄ nanoparticles decorated smectite nanocomposite: Characterization, photocatalytic and electrocatalytic activities. *Solid State Sci.* **2018**, *83*, 122–136. [[CrossRef](#)]
43. Guo, Y.; Yu, W.; Chen, J.; Wang, X.; Gao, B.; Wang, G. Ag₃PO₄/rectorite nanocomposites: Ultrasound-assisted preparation, characterization and enhancement of stability and visible-light photocatalytic activity. *Ultrason. Sonochem.* **2017**, *34*, 831–838. [[CrossRef](#)] [[PubMed](#)]
44. Valášková, M.; Tokarský, J.; Pavlovský, J.; Prostějovský, T.; Kočí, K. α-Fe₂O₃ Nanoparticles/Vermiculite Clay Material: Structural, Optical and Photocatalytic Properties. *Materials* **2019**, *12*, 1880. [[CrossRef](#)] [[PubMed](#)]
45. Araujo, F.P.; Trigueiro, P.; Honório, L.M.C.; Furtini, M.B.; Oliveira, D.M.; Almeida, L.C.; Garcia, R.R.P.; Viana, B.C.; Silva-Filho, E.C.; Osajima, J.A. A novel green approach based on ZnO nanoparticles and polysaccharides for photocatalytic performance. *Dalton Trans.* **2020**, *49*, 16394–16403. [[CrossRef](#)] [[PubMed](#)]
46. Araujo, F.P.; Trigueiro, P.; Honório, L.M.; Oliveira, D.M.; Almeida, L.C.; Garcia, R.P.; Lobo, A.O.; Cantanhêde, W.; Silva-Filho, E.C.; Osajima, J.A. Eco-friendly synthesis and photocatalytic application of flowers-like ZnO structures using Arabic and Karaya Gums. *Int. J. Biol. Macromol.* **2020**, *165*, 2813–2822. [[CrossRef](#)] [[PubMed](#)]
47. Goktas, A.; Modanlı, S.; Tumbul, A.; Kilic, A. Facile synthesis and characterization of ZnO, ZnO:Co, and ZnO/ZnO:Co nano rod-like homojunction thin films: Role of crystallite/grain size and microstrain in photocatalytic performance. *J. Alloys Compd.* **2021**, *893*, 162334. [[CrossRef](#)]
48. Mustapha, S.; Ndamitso, M.M.; Abdulkareem, A.S.; Tijani, J.O.; Shuaib, D.T.; Ajala, A.O.; Mohammed, A.K. *Application of TiO₂ and ZnO Nanoparticles Immobilized on Clay in Wastewater Treatment: A Review*; Springer International Publishing: Berlin/Heidelberg, Germany, 2020; Volume 10, ISBN 0123456789.
49. Peng, H.; Liu, X.; Tang, W.; Ma, R. Facile synthesis and characterization of ZnO nanoparticles grown on halloysite nanotubes for enhanced photocatalytic properties. *Sci. Rep.* **2017**, *7*, 2250. [[CrossRef](#)]
50. Misra, A.J.; Das, S.; Rahman, A.H.; Das, B.; Jayabalan, R.; Behera, S.K.; Suar, M.; Tamhankar, A.J.; Mishra, A.; Lundborg, C.S.; et al. Doped ZnO nanoparticles impregnated on Kaolinite (Clay): A reusable nanocomposite for photocatalytic disinfection of multidrug resistant *Enterobacter* sp. under visible light. *J. Colloid Interface Sci.* **2018**, *530*, 610–623. [[CrossRef](#)]
51. Liu, J.; Dong, M.; Zuo, S.; Yu, Y. Solvothermal preparation of TiO₂/montmorillonite and photocatalytic activity. *Appl. Clay Sci.* **2009**, *43*, 156–159. [[CrossRef](#)]
52. Hadjltaief, H.B.; Galvez, M.E.; Ben Zina, M.; Da Costa, P. TiO₂/clay as a heterogeneous catalyst in photocatalytic/photochemical oxidation of anionic reactive blue 19. *Arab. J. Chem.* **2019**, *12*, 1454–1462. [[CrossRef](#)]
53. Gombos, E.D.; Krakkó, D.; Zárny, G.; Illés, A.; Dóbe, S.; Szegedi, Á. Laponite immobilized TiO₂ catalysts for photocatalytic degradation of phenols. *J. Photochem. Photobiol. A Chem.* **2019**, *387*, 112045. [[CrossRef](#)]
54. El Gaidoumi, A.; Rodríguez, J.M.D.; Melián, E.P.; González-Díaz, O.M.; Santos, J.A.N.; El Bali, B.; Kherbeche, A. Synthesis of sol-gel pyrophyllite/TiO₂ heterostructures: Effect of calcination temperature and methanol washing on photocatalytic activity. *Surf. Interfaces* **2018**, *14*, 19–25. [[CrossRef](#)]
55. Belver, C.; Bedia, J.; Rodriguez, J. Zr-doped TiO₂ supported on delaminated clay materials for solar photocatalytic treatment of emerging pollutants. *J. Hazard. Mater.* **2017**, *322*, 233–242. [[CrossRef](#)] [[PubMed](#)]
56. Belver, C.; Han, C.; Rodriguez, J.; Dionysiou, D. Innovative W-doped titanium dioxide anchored on clay for photocatalytic removal of atrazine. *Catal. Today* **2017**, *280*, 21–28. [[CrossRef](#)]
57. Akkari, M.; Aranda, P.; Amara, A.B.H.; Ruiz-Hitzky, E. Clay-Nanoarchitectures as Photocatalysts by In Situ Assembly of ZnO Nanoparticles and Clay Minerals. *J. Nanosci. Nanotechnol.* **2018**, *18*, 223–233. [[CrossRef](#)] [[PubMed](#)]
58. Akkari, M.; Aranda, P.; Belver, C.; Bedia, J.; Amara, A.B.H.; Ruiz-Hitzky, E. ZnO/sepiolite heterostructured materials for solar photocatalytic degradation of pharmaceuticals in wastewater. *Appl. Clay Sci.* **2018**, *156*, 104–109. [[CrossRef](#)]

59. Shi, Y.; Hu, Y.; Zhang, L.; Yang, Z.; Zhang, Q.; Cui, H.; Zhu, X.; Wang, J.; Chen, J.; Wang, K. Palygorskite supported BiVO₄ photocatalyst for tetracycline hydrochloride removal. *Appl. Clay Sci.* **2017**, *137*, 249–258. [[CrossRef](#)]
60. Huo, C.; Yang, H. Preparation and enhanced photocatalytic activity of Pd–CuO/palygorskite nanocomposites. *Appl. Clay Sci.* **2013**, *74*, 87–94. [[CrossRef](#)]
61. Zhang, Y.; Yang, H. Co₃O₄ nanoparticles on the surface of halloysite nanotubes. *Phys. Chem. Miner.* **2012**, *39*, 789–795. [[CrossRef](#)]
62. Guo, Y.; Li, C.; Guo, Y.; Wang, X.; Li, X. Ultrasonic-assisted synthesis of mesoporous g-C₃N₄/Na-bentonite composites and its application for efficient photocatalytic simultaneous removal of Cr(VI) and RhB. *Colloids Surf. A Physicochem. Eng. Asp.* **2019**, *578*, 123624. [[CrossRef](#)]
63. Wang, J.; Fan, J.; Li, J.; Wu, X.; Zhang, G. Ultrasound assisted synthesis of Bi₂NbO₅F/rectorite composite and its photocatalytic mechanism insights. *Ultrason. Sonochem.* **2018**, *48*, 404–411. [[CrossRef](#)]
64. Wang, X.; Mu, B.; Hui, A.; Wang, A. Comparative study on photocatalytic degradation of Congo red using different clay mineral/CdS nanocomposites. *J. Mater. Sci. Mater. Electron.* **2019**, *30*, 5383–5392. [[CrossRef](#)]
65. Zou, Y.; Hu, Y.; Shen, Z.; Yao, L.; Tang, D.; Zhang, S.; Wang, S.; Hu, B.; Zhao, G.; Wang, X. Application of aluminosilicate clay mineral-based composites in photocatalysis. *J. Environ. Sci.* **2022**, *115*, 190–214. [[CrossRef](#)] [[PubMed](#)]
66. Lopes, J.D.S.; Rodrigues, W.V.; Oliveira, V.V.; Braga, A.D.N.S.; da Silva, R.T.; França, A.A.C.; da Paz, E.C.; Osajima, J.A.; Filho, E.C.D.S. Modification of kaolinite from Pará/Brazil region applied in the anionic dye photocatalytic discoloration. *Appl. Clay Sci.* **2018**, *168*, 295–303. [[CrossRef](#)]
67. Zyoud, A.H.; Asaad, S.; Zyoud, S.H.; Zyoud, S.H.; Helal, M.H.; Qamhieh, N.; Hajamohideen, A.; Hilal, H.S. Raw clay supported ZnO nanoparticles in photodegradation of 2-chlorophenol under direct solar radiations. *J. Environ. Chem. Eng.* **2020**, *8*, 104227. [[CrossRef](#)]
68. Tun, P.P.; Wang, J.; Khaing, T.T.; Wu, X.; Zhang, G. Fabrication of functionalized plasmonic Ag loaded Bi₂O₃/montmorillonite nanocomposites for efficient photocatalytic removal of antibiotics and organic dyes. *J. Alloys Compd.* **2019**, *818*, 152836. [[CrossRef](#)]
69. Karaevvaz, M.C.; Balci, S. One pot synthesis of aluminum pillared intercalated layered clay supported silicotungstic acid (STA/Al-PILC) catalysts. *Microporous Mesoporous Mater.* **2021**, *323*, 111193. [[CrossRef](#)]
70. Gil, A.; Gandía, L.M.; Vicente, M.A. Recent Advances in the Synthesis and Catalytic Applications of Pillared Clays. *Catal. Rev.-Sci. Eng.* **2000**, *42*, 145–212. [[CrossRef](#)]
71. Bergaya, F.; Aouad, A.; Mandalia, T. Chapter 7.5 Pillared Clays and Clay Minerals. *Dev. Clay Sci.* **2006**, *1*, 393–421. [[CrossRef](#)]
72. Pandey, P.; Saini, V.K. Pillared interlayered clays: Sustainable materials for pollution abatement. *Environ. Chem. Lett.* **2018**, *17*, 721–727. [[CrossRef](#)]
73. Gil, A.; Vicente, M.A. Progress and perspectives on pillared clays applied in energetic and environmental remediation processes. *Curr. Opin. Green Sustain. Chem.* **2019**, *21*, 56–63. [[CrossRef](#)]
74. Yang, J.-H.; Piao, H.; Vinu, A.; Elzatahry, A.A.; Paek, S.-M.; Choy, J.-H. TiO₂-pillared clays with well-ordered porous structure and excellent photocatalytic activity. *RSC Adv.* **2014**, *5*, 8210–8215. [[CrossRef](#)]
75. Abdennouri, M.; Baálala, M.; Galadi, A.; El Makhfouk, M.; Bensitel, M.; Nohair, K.; Sadiq, M.; Boussaoud, A.; Barka, N. Photocatalytic degradation of pesticides by titanium dioxide and titanium pillared purified clays. *Arab. J. Chem.* **2016**, *9*, S313–S318. [[CrossRef](#)]
76. Kim, D.-S.; Lee, D.-K. Low-temperature catalytic aqueous phase oxidation of microcystin-LR with iron-doped TiO₂ pillared clay catalysts. *Environ. Technol.* **2020**, *42*, 3546–3553. [[CrossRef](#)] [[PubMed](#)]
77. Hadj Bachir, D.; Khalaf, H.; Ferroukhi, S.; Boutoumi, Y.; Schnee, J.; Gaigneaux, E.M. Preparation and Characterization of TiO₂ Pillared Clay: Effect of Palladium and Photosensitizer on Photocatalytic Activity. *Res. J. Chem. Environ.* **2019**, *24*, 60–73.
78. González, B.; Trujillano, R.; Vicente, M.A.; Rives, V.; Korili, S.A.; Gil, A. Photocatalytic degradation of trimethoprim on doped Ti-pillared montmorillonite. *Appl. Clay Sci.* **2019**, *167*, 43–49. [[CrossRef](#)]
79. Silva, A.S.; Kalmakhanova, M.S.; Massalimova, B.K.; Sgorlon, J.G.; Luis, D.D.T.J.; Gomes, H.T. Wet Peroxide Oxidation of Paracetamol Using Acid Activated and Fe/Co-Pillared Clay Catalysts Prepared from Natural Clays. *Catalysts* **2019**, *9*, 705. [[CrossRef](#)]
80. Xu, T.; Zhu, R.; Zhu, J.; Liang, X.; Liu, Y.; Xu, Y.; He, H. Ag₃PO₄ immobilized on hydroxy-metal pillared montmorillonite for the visible light driven degradation of acid red 18. *Catal. Sci. Technol.* **2016**, *6*, 4116–4123. [[CrossRef](#)]
81. Baloyi, J.; Ntho, T.; Moma, J. Synthesis of highly active and stable Al/Zr pillared clay as catalyst for catalytic wet oxidation of phenol. *J. Porous Mater.* **2018**, *26*, 583–597. [[CrossRef](#)]
82. Bouna, L.; Rhouta, B.; Amjoud, M.; Maury, F.; Lafont, M.-C.; Jada, A.; Senocq, F.; Daoudi, L. Synthesis, characterization and photocatalytic activity of TiO₂ supported natural palygorskite microfibers. *Appl. Clay Sci.* **2011**, *52*, 301–311. [[CrossRef](#)]
83. Akkari, M.; Aranda, P.; Ben Rhaïem, H.; Amara, A.B.H.; Ruiz-Hitzky, E. ZnO/clay nanoarchitectures: Synthesis, characterization and evaluation as photocatalysts. *Appl. Clay Sci.* **2016**, *131*, 131–139. [[CrossRef](#)]
84. Zhou, F.; Yan, C.; Liang, T.; Sun, Q.; Wang, H. Photocatalytic degradation of Orange G using sepiolite-TiO₂ nanocomposites: Optimization of physicochemical parameters and kinetics studies. *Chem. Eng. Sci.* **2018**, *183*, 231–239. [[CrossRef](#)]
85. Zhou, F.; Yang, M.; Lu, R.; Yan, C. Simultaneous adsorption-photocatalytic treatment with TiO₂-Sep nanocomposites for in situ remediation of sodium pentachlorophenol contaminated aqueous and soil. *Environ. Sci. Pollut. Res.* **2022**, *29*, 39557–39566. [[CrossRef](#)] [[PubMed](#)]

86. Messaoudi, Z.A.; Lahcene, D.; Benaissa, T. Adsorption and Photocatalytic Degradation of Crystal Violet Dye under Sunlight Irradiation Using Natural and Modified Clays by Zinc Oxide. *Chem. Methodol.* **2022**, *6*, 661–676. [[CrossRef](#)]
87. Lazaar, K.; Chargui, H.; Pullar, R.; Hajjaji, W.; Moussi, B.; Labrincha, J.; Rocha, F.; Jamoussi, F. Efficiency of natural clay and titania P25 composites in the decolouring of methylene blue (MB) from aqueous solutions: Dual adsorption and photocatalytic processes. *Arab. J. Geosci.* **2021**, *14*, 400. [[CrossRef](#)]
88. Chkirida, S.; Zari, N.; Achour, R.; Hassoune, H.; Lachehab, A.; Qaiss, A.E.K.; Bouhfid, R. Highly synergic adsorption/photocatalytic efficiency of Alginate/Bentonite impregnated TiO₂ beads for wastewater treatment. *J. Photochem. Photobiol. A Chem.* **2021**, *412*, 113215. [[CrossRef](#)]
89. Huang, M.; Xu, C.; Wu, Z.; Huang, Y.; Lin, J.; Wu, J. Photocatalytic discolorization of methyl orange solution by Pt modified TiO₂ loaded on natural zeolite. *Dye. Pigment.* **2008**, *77*, 327–334. [[CrossRef](#)]
90. van Grieken, R.; Aguado, J.; López-Muñoz, M.; Marugán, J. Synthesis of size-controlled silica-supported TiO₂ photocatalysts. *J. Photochem. Photobiol. A Chem.* **2002**, *148*, 315–322. [[CrossRef](#)]
91. Martins, A.C.; Cazetta, A.L.; Pezoti, O.; de Souza, J.R.B.; Zhang, T.; Pilau, E.; Asefa, T.; Almeida, V.C. Sol-gel synthesis of new TiO₂/activated carbon photocatalyst and its application for degradation of tetracycline. *Ceram. Int.* **2017**, *43*, 4411–4418. [[CrossRef](#)]
92. Wang, D.; Jia, F.; Wang, H.; Chen, F.; Fang, Y.; Dong, W.; Zeng, G.; Li, X.; Yang, Q.; Yuan, X. Simultaneously efficient adsorption and photocatalytic degradation of tetracycline by Fe-based MOFs. *J. Colloid Interface Sci.* **2018**, *519*, 273–284. [[CrossRef](#)]